ELSEVIER

European Polymer Journal 37 (2001) 2159–2168

EUROPEAN POLYMER JOURNAL

www.elsevier.com/locate/europolj

Physical properties of thermoplastic/graphite composites

I. Krupa, I. Chodák *

Polymer Institute, Slovak Academy of Science, Dubravska cesta 9, 8242 36 Bratislava, Slovakia

Received 11 March 2001; accepted 10 April 2001

Abstract

Thermal and electrical conductivity, thermal diffusivity of high density polyethylene, polystyrene/graphite composites were investigated in this paper. Two different types of graphite (different distribution of the particle size, different specific surface) were used. For HDPE/graphite composites, also mechanical properties were investigated. Experimental data were compared with some theoretical models. In a semicrystalline matrix (HDPE) different values for the percolation concentration for two types of graphite particles of different surface area were observed. © 2001 Elsevier Science Ltd. All rights reserved.

Keywords: Polyethylene; Polystyrene/graphite composites; Thermal conductivity; Thermal diffusivity; Electrical conductivity; Mechanical properties

1. Introduction

Polymer/graphite composites have long been used in structural, aerospace and sporting goods applications. In recent years, increasing attention has been devoted to developing polymer/graphite composites for applications where electrical conductivity, or thermal conductivity is required [1–3].

Electroconductive composites are often used as heating elements, temperature-dependent resistors and sensors, self-limiting electrical heaters and switching devices, antistatic materials for electromagnetic interference shielding of electronic devices etc. [4].

The importance of thermal conductivity and/or thermal diffusivity in polymer composites is associated with the need for appreciable levels of thermal conductance in circuit boards, heat exchangers, appliances, and machinery [5]. The information on these parameters of materials is also necessary for modelling the optimum conditions during processing of materials, as well as for an analysis of transport of heat in materials during practical applications. Since many materials are also mechanically strained, the data concerning ultimate especially mechanical properties e.g. Young's modulus are very useful for any considerations on the application of the material.

2. Experimental

Two grades of thermoplastics were used as the matrix, namely high density polyethylene (HDPE BP 5740 3VA, British Petroleum, UK) and polystyrene (Krasten 127, Kaučuk a.s., Cz, MFI = 15–20 g/10 min) while two grades graphite (EG-10, synthetic graphite, SGL Carbon, UK and KS-15, synthetic graphite, Lonza, Switzerland) were used as the fillers.

The blends were prepared by mixing both components in a 50 ml mixing chamber of Brabender Plasticorder PLE 331 at 170°C (PS) or 200°C (HDPE) for 10 min at the mixing speed 35 rpm.

For the electrical conductivity measurements the prepared composites were compression moulded using a laboratory press Fontijne 200 (The Netherland) at 170°C (PS) or 200°C (HDPE) for 2 min under 22.5 $\mathrm{kN\,cm^{-2}}$. The thickness of the compression moulded samples was about 0.2 mm. The volume electrical conductivity

---

* Corresponding author.
E-mail address: upolchiv@savba.sk (I. Chodák).

0014-3057/01/$ - see front matter © 2001 Elsevier Science Ltd. All rights reserved.
PII: S0014-3057(01)00115-X

in polymer composites was measured according to ASTM D 257. Three electrode electrometer arrangement was used for the DC-measurement of the resistance. The voltage level used varied in the range 0.1–500 V. Electroconductive solution was used to achieve good electrical contacts between the sample surface and the electrode of the conduction tester.

For thermal conductivity and thermal diffusivity measurements the specimens with 50 mm diameter and 10 mm thick have been compression moulded at 170°C or 200°C for 5 min with subsequent cooling under the pressure down to 70°C.

The thermal conductivities were measured using a newly developed multipurpose apparatus (ISOMET, Applied Precision, Bratislava, Slovakia) for nonsteady state measurement of thermal properties. The data have been calculated automatically from the analysis of a time dependence of the thermal flow in the material. Measurements have been made at 25 ± 2°C using a flat probe.

The crystallinity of the samples was measured using a Perkin–Elmer DSC 2 at heating rate 10°C min^{-1} as a second melting run after normalised crystallisation at cooling rate 10°C min^{-1}.

The distribution of the size of particles were determined by Sympatec Helos (H0367) from the measurements of the sedimentation of the particles in water.

The shape of particles of graphite was determined by scanning electron microscopy (Tesla BM 5545, Czech Republic).

3. Results and discussion

3.1. Characterisation of the graphite particles

In our experiments, two different types of graphite were used. Their granulometric parameters are summarised in Table 1. The curves of differential and integral volume distributions are shown in Fig. 1. Photographs of the particles are shown in Figs. 2 and 3.

From Table 1, as well as from Fig. 1 it seen that graphite KS has smaller particles, more narrow particle size distribution as well as higher specific surface than graphite EG.

Figs. 2 and 3 indicate that particles of both types of graphite are irregularly shaped and contain many sharp edges.

Table 1

Granulometric parameters of particles of graphite EG and KS

Type	x_{10} (µm)	x_{16} (µm)	x_{50} (µm)	x_{84} (µm)	x_{90} (µm)	x_{99} (µm)	S_v (m^2 g^{-1})
Graphite KS	6.6	8.0	14.1	24.1	28.4	48.0	0.245
Graphite EG	10.9	14.0	31.6	59.1	69.2	108.0	0.125

x_i – i% of volume of particles is smaller than dimension x_i.

S_v: Specific surface of particles.

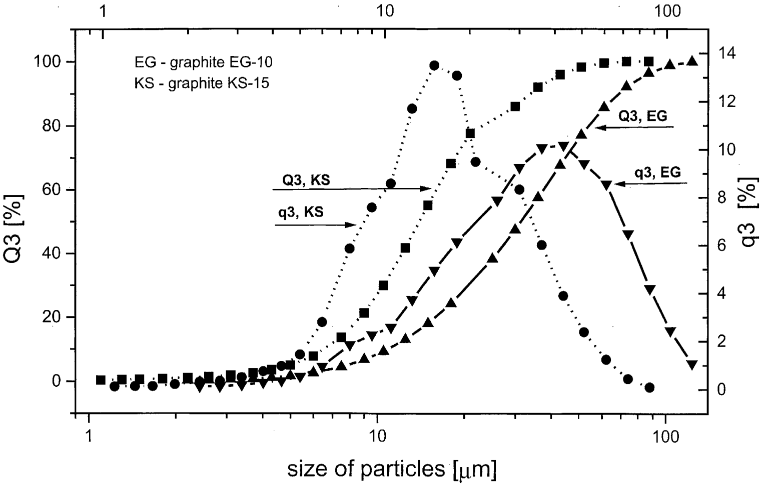

Fig. 1. Differential distribution of the particle size of graphite KS (●), graphite EG (▼) and integral distribution of the particle size of graphite KS (■), graphite EG (▲).

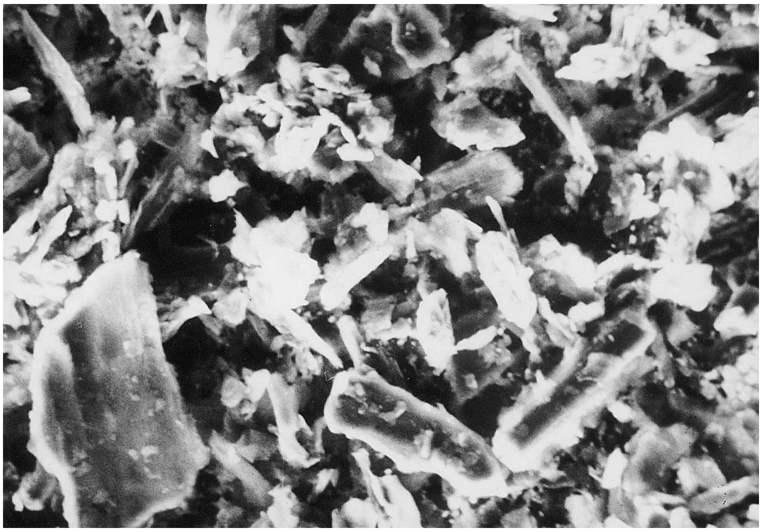

Fig. 2. SEM micrograph of graphite EG particles (magnification 500×).

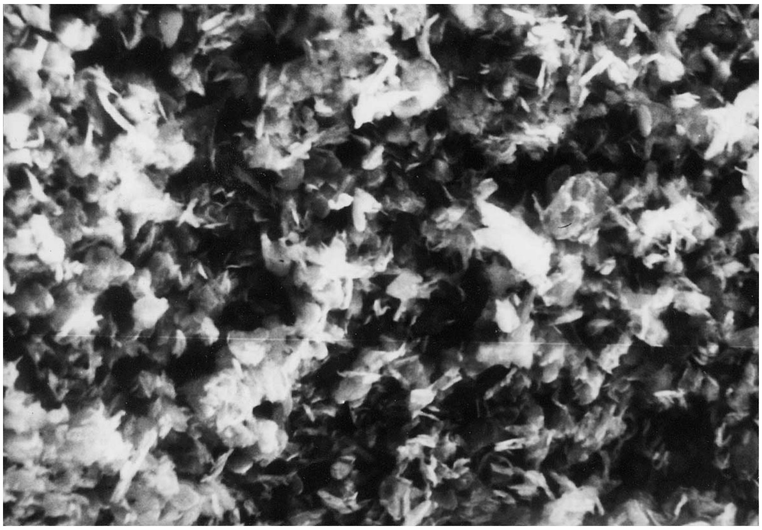

Fig. 3. SEM micrograph of graphite KS particles (magnification 500×).

3.2. Electrical conductivity

The dependencies of electrical conductivity of composites HDPE, PS/graphite composites versus volume portion of the filler are shown in Figs. 4 and 5.

In all cases, a dramatical increase of electrical conductivity was observed around a particular concentration of the filler. This concentration is generally called percolation concentration. In this case, at least one infinite cluster of particles is formed in polymeric matrix. This cluster penetrates throughout the sample while the particles in the cluster are in close contact and represent a conductive path for a movement of electrons throughout the sample. Obviously, in a real situation, when only limited number of experimental points is available, the unambiguous determination of exact percolation concentration is difficult. To solve this problem, percolation point has been arbitrary identified as an inflexion point in an empirical fitting curve. For a fitting of experimental data we suggested Eq. (1) [6]:

$$\log(\sigma_c/\sigma_m) = B(1 - e^{-a\phi_f})^n \qquad (1)$$

where B, a, n are adjustable parameters, σ_c is electrical conductivity of composites, σ_m is electrical conductivity

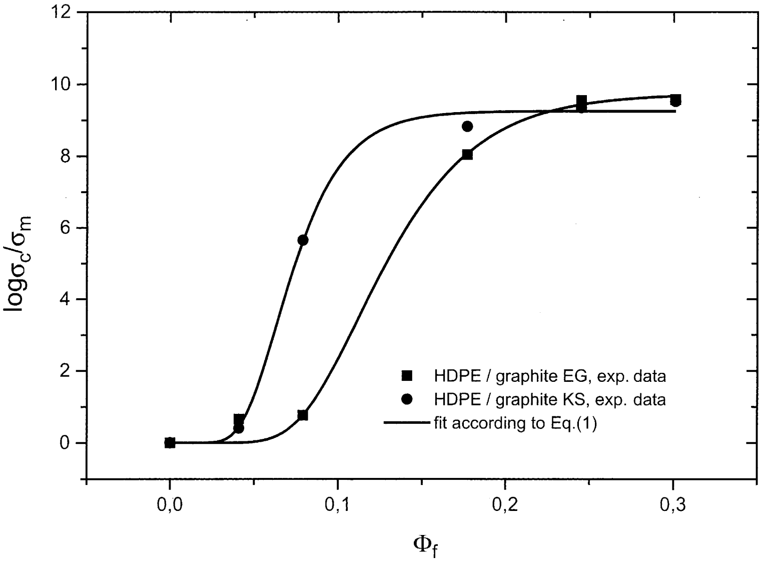

Fig. 4. Relative electrical conductivity (σ_c/σ_m) of the graphite EG (■) and graphite KS (●) filled HDPE graphite on the volume filler content (ϕ_f). Solid lines – curve fitting (Eq. (1)).

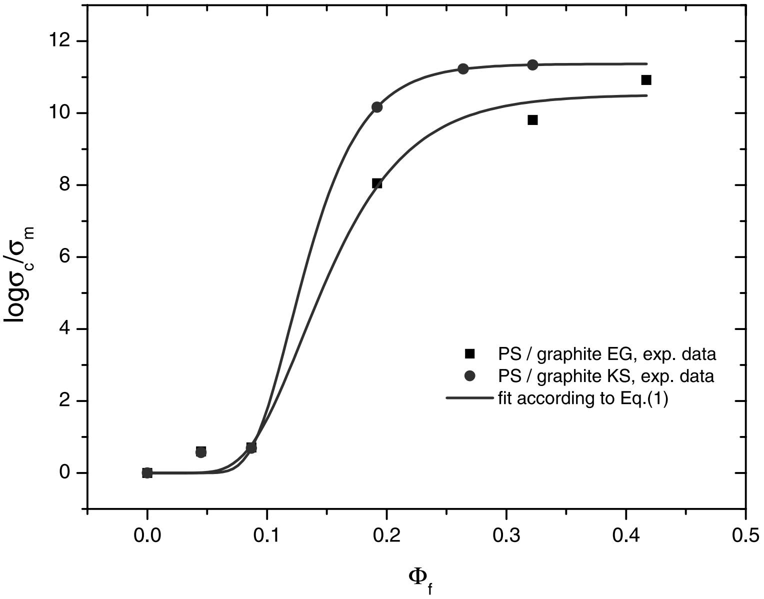

Fig. 5. Relative electrical conductivity (σ_c/σ_m) of the graphite EG (■) and graphite KS (●) filled PS graphite on the volume filler content (ϕ_f). Solid lines – curve fitting (Eq. (1)).

of polymeric matrix and ϕ_f is volume portion of the filler.

An inflexion point (ϕ_i) is calculated according to Eq. (2). This point is identified with percolation concentration (ϕ_c).

$$\phi_i \equiv \phi_c = \ln(n)/a \tag{2}$$

Percolation concentration of investigated composites, as well as parameters B, a, n are summarised in Table 2.

It is seen that parameter B can be approximately expressed as:

$$B \cong \log(\sigma_{c,\max}/\sigma_m) \tag{3}$$

Table 2
The values of parameters in Eq. (1): B, a, n, percolation concentration (ϕ_c), calculated according to Eq. (2), maximum experimentally determined value of electrical conductivity of composites ($\sigma_{c,\max}$), electrical conductivity of matrix (σ_m)

Composite	B	a	n	ϕ_c	$\log(\sigma_{c,\max}/\sigma_m)$
HDPE/EG	9.8 (0.4)	25.8 (4.5)	18.3 (9.3)	0.11	10.3
HDPE/KS	9.3 (0.2)	45.8 (6.7)	18.3 (9.1)	0.06	9.5
PS/EG	10.5 (0.4)	20.5 (4.0)	14.2 (8.4)	0.13	10.9
PS/KS	11.4 (0.3)	30.4 (4.3)	38.0 (18.4)	0.12	11.3

Values in brackets are standard deviations.

where $\sigma_{c,\max}$ is a maximum value of electrical conductivity of composites at maximum experimental concentration of the filler.

Experimental results (Table 2, Figs. 4 and 5) show that different types of graphite have a different influence on the percolation concentration of composites.

If PS matrix is used, the percolation concentrations are similar for both types of graphite. It means, that percolation concentration does not depend on the size of particles nor on its distribution. This fact is in agreement with theoretical preconditions. Percolation concentration strongly depends on a shape of particles, but should not depend on the size of particles [7]. However, if HDPE matrix was used, we observed that HDPE/graphite KS composites showed much lower percolation concentration than HDPE/graphite EG composites. This behaviour can be caused by an agglomeration of particles. Amorphous part of HDPE matrix is 30% (Table 3). Obviously, particles can be distributed only in this part of matrix. Since particles of graphite KS are smaller and have higher specific surface, they can agglomerate easier than bigger particles of graphite EG. Considering that a random statistic distribution of particles in matrix is accompanied by an agglomeration process (strictly theoretically, percolation is purely geometrical concept), then infinite cluster can be created at lower concentration of particles.

3.3. Thermal conductivity of composites

The thermal conductivities of HDPE, PS/graphite composites versus graphite content are shown in Figs. 6 and 7. A nonlinear increase of thermal conductivities was observed with an increase in graphite content. It is interesting that thermal conductivities of composites filled with graphite KS are higher than thermal conductivities of material filled with the same concentration of graphite EG. This difference is more significant for PS matrix, especially at higher filler concentrations. Since thermal conductivities should not depend on the size of particles [5,8], the most probable explanation is that more conductive paths is created as a consequence of higher agglomeration of particles of graphite KS, similarly to the electrical conductivity as discussed above.

Many different models have been already developed for descriptions of thermal conductivity of composites [5,8] but none of them has general validity. The models can be divided into three groups. The first is based on an exact approach to the problem of transport of heat using an effective medium approximation, the second one deals with a calculation of upper and lower boundaries and the last one is developed on the bond percolation theory [9]. The models, based on the effective medium approximation as well as bonds calculations often fails, if thermal conductivity of the filler is substantially different of that of matrix (by more than one order of magnitude). This is also the case for other properties [10]. Therefore, percolation models have attracted a special attention recently [9,11]. An elegant percolation model of thermal conductivities has been presented by Bujard et al. [9]. Unfortunately, this model is not directly applicable for our systems, since they do not fulfil preconditions considered by the authors.

Other known model, which correlates thermal conductivity with an ability of the filler to create infinity clusters of particles is model of Agari et al. [12,13] and Wunderlich [14]. The thermal conductivity is generally described by Eq. (4):

Table 3
The specific melting enthalpy (ΔH_m), melting temperature (T_m), degree of crystallinity (w_c) and values of the relative change of degree of crystallinity (δw_c) of HDPE and composites

Sample	ΔH_m (J g^{-1})	T_m (°C)	w_c[a] (%)	$\delta w_c \times 100$ (%)
HDPE	198.89	129.3	69.1	–
H60KS	207.32	127.9	72.0	4.2
H60EG	205.83	128.7	71.5	3.5

[a] Values of w_c are calculated according to Eq. (5), $\Delta H_m^+ = 288$ J g^{-1}; H60EG–HDPE + 60 wt.% of graphite EG, H60KS–HDPE + 60 wt.% of graphite KS.

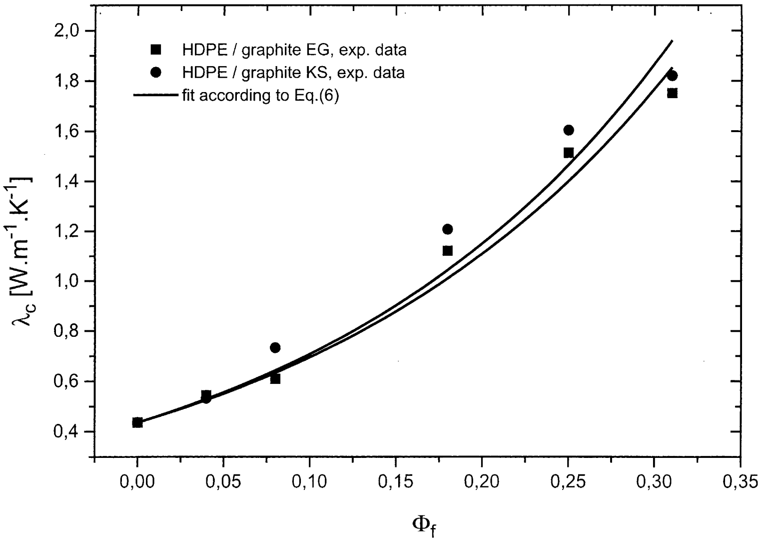

Fig. 6. Thermal conductivity (λ_c) of the graphite EG (■) and graphite KS (●) filled HDPE graphite on the volume filler content (ϕ_f). Solid lines – curve fitting (Eq. (6)).

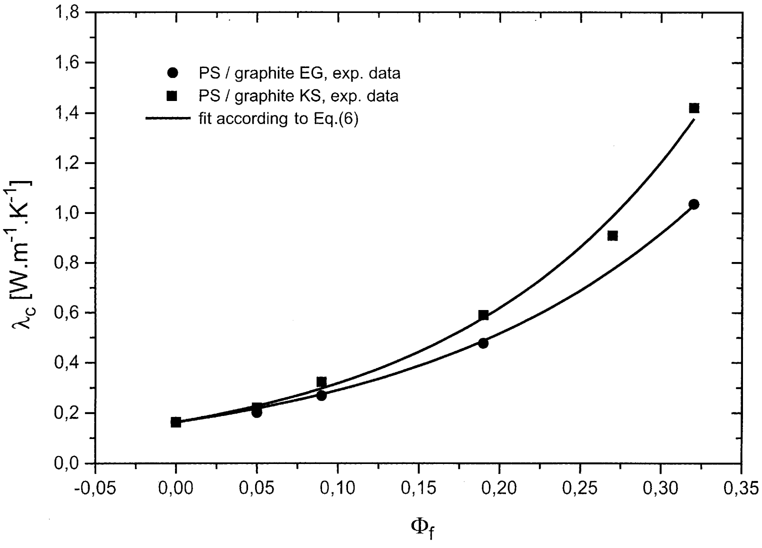

Fig. 7. Thermal conductivity (λ_c) of the graphite EG (■) and graphite KS (●) filled PS graphite on the volume filler content (ϕ_f). Solid lines – curve fitting (Eq. (6)).

$$\log \lambda_c = \phi_f c_2 \log \lambda_f + (1 - \phi_f) \log(c_1 \lambda_m) \tag{4}$$

where λ_c, λ_m, λ_f are thermal conductivities of composite, matrix and filler, ϕ_f is volume portion of the filler and parameter c_2 characterises the ability of the filler particles to create infinite cluster. Parameter c_1 is related to the change of thermal conductivity of semicrystalline matrix, as a consequence of change of degree of crystallinity. In order to check this influence, we determined specific melting enthalpy of HDPE as well as composite filled with 60% of graphite (Table 3). Degree of crystallinity was calculated according to Eq. (5):

$$w_c = \frac{\Delta H_m}{\Delta H_m^+} \tag{5}$$

where ΔH_m is specific melting enthalpy of polyethylene and $\Delta H_m^+ = 288$ J g^{-1} [14] is specific melting enthalpy for 100% crystalline polyethylene. From the data in Table 3 it is clear that a change of crystallinity of HDPE is relatively small and probably does not influence the thermal conductivity of polymeric matrix. In this case, parameter $c_1 = 1$ and Eq. (4) can be transformed as [13]:

$$\log \frac{\lambda_c}{\lambda_m} = \phi_f c_2 \log \frac{\lambda_f}{\lambda_m} \tag{6}$$

The authors showed correlations between parameter c_2 and percolation concentration for some composites:

$$c_2 = \log(1/\phi_c^A) \tag{7}$$

In this case, the percolation concentration is marked as ϕ_c^A.

Eq. (6) was applied to our experimental data. Parameters c_2 and ϕ_c^A are summarised in Table 4. We can conclude that if parameter c_2 is the only adjustable parameter, Eq. (6) fits the experimental data quite well (Figs. 6 and 7) but correlation between percolation concentration, determined from electrical conductivities measurements and percolation concentration calculated according to Eq. (7) is not very good. Strictly speaking, this model is not a percolation model with general validity, since it just represents a correlation between thermal conductivity and percolation concentration.

3.4. Thermal diffusivity

Thermal diffusivity (k) is transport coefficient which is related to microscopic transport of heat. This value is directly associated with a change of temperature of material. Thermal diffusivity generally depends on pressure and temperature and in the case of composites depend also on the filler concentration.

Table 4
Parameters in Agari et al. model: Eq. (6)

Composite	λ_f/λ_m [a]	c_2	ϕ_c^A
HDPE/EG	477.8	0.739 (0.057)	0.18
HDPE/KS	477.8	0.843 (0.086)	0.14
PS/EG	1247.3	0.818 (0.063)	0.15
PS/KS	1247.3	0.920 (0.049)	0.12

Values in the brackets are standard deviations.
[a] $\lambda_f = 208.3\ \mathrm{W\,m^{-1}\,K^{-1}}$ [12].

The thermal diffusivities of PS/graphite EG, PS/graphite KS, HDPE/graphite EG, HDPE/graphite KS as a function of graphite content are depicted in Fig. 8.

A nonlinear increase of thermal diffusivities with an increase in graphite content is observed in all cases. Inorganic fillers have much higher thermal diffusivity than polymers and therefore improve thermal diffusivity of composites.

An increase of thermal diffusivity of composites with an increase of thermal diffusivity of polymeric matrix at the same filler concentration is also observed. The thermal diffusivity of HDPE is higher than thermal diffusivity of PS. The same is true for their thermal conductivities. Semicrystalline matrices have higher both thermal conductivity and thermal diffusivity compared to amorphous matrices, since crystalline phase (regular structure) enables a better transport of heat than amorphous phase.

It is seen (Fig. 8) that composites filled with graphite KS have higher thermal diffusivity than composite filled with graphite EG at the same concentration. Since thermal diffusivity of both types of graphite is the same

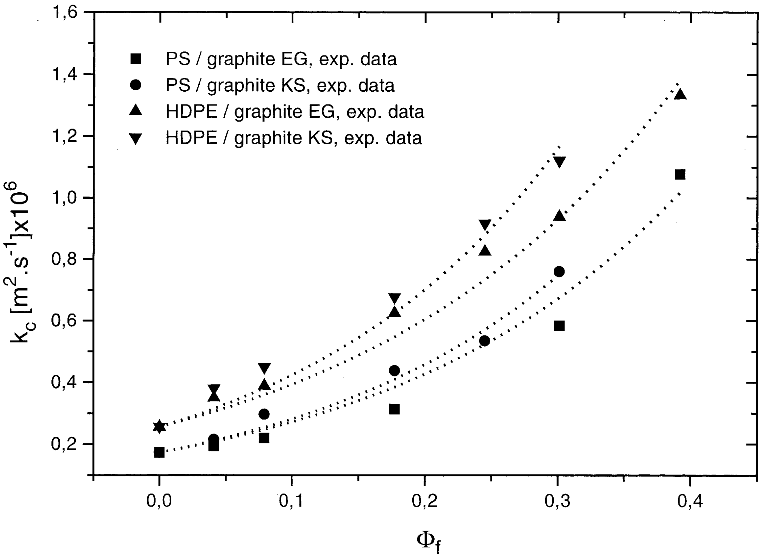

Fig. 8. Thermal diffusivity (k_c) of the graphite EG (■), graphite KS (●) filled PS and thermal diffusivity of the graphite EG (▲), graphite KS (▼) filled HDPE versus the volume filler content (ϕ_f).

($\approx 123 \times 10^{-6}$ m^2 s^{-1}, at 25°C), we assume that this fact is caused by higher aggregation of smaller graphite KS particles. The aggregates could improve a heat transport in the materials and improve thermal diffusivity, similarly as discussed above for thermal conductivity.

3.5. Mechanical properties

3.5.1. Young's modulus of elasticity

Dependencies for Young's modulus of composites versus volume portion of the filler are shown in the Fig. 9. It is seen that Young's modulus increases with an increase in a filler content in all concentration region. The increase is more pronounced for HDPE filled with graphite KS than if graphite EG was used at the same concentration. This fact is associated with the higher specific surface of the particles of graphite KS, since the interactions between components are more intensive in this case.

3.5.2. Elongation at break

The dependencies of elongation at break versus graphite content are shown in Fig. 10. We observed a dramatical decrease of elongation at break with an increase in graphite content for both investigated systems.

Generally, a decrease of elongation at break with an increase in filler content is always observed. For description of this behaviour, a few models have been suggested. The most known of them is Nielsen's model [15] given by Eq. (8):

$$\frac{\varepsilon_{b,c}}{\varepsilon_{b,m}} = 1 - \phi_f^{1/3} \qquad (8)$$

where $\varepsilon_{b,m}$ is elongation at break of matrix and ϕ_f is volume portion of filler. This model is valid if particles have spherical shape assuming perfect adhesion between phases. Many fillers do not fulfil these conditions. As seen in Figs. 2 and 3, our graphites has very irregular shape. Particles consist of many sharp edges. Moreover, particles are not uniform. These geometrical factors are expected to contribute significantly to a dramatic decrease of elongation at break.

It is worth to display values of the coefficient of variance of elongation at break versus graphite content (Table 5). We can see that the biggest scatter of elongation at break has been observed at the lowest filler concentrations. The presence of a filler in the matrix results, besides a reinforcing effect, also in a formation of sites of stress concentration. If the filler content is low, the number of these sites is small and their size is below the critical size above which a rapid crack growth occurs. Therefore the deformation of the composite with a ductile matrix is high and coefficient of variance is within expected limits. At high filler content, the number of stress concentrating sites is high, they are in close vicinity and the crack, once formed, can propagate rapidly through the sample. Besides this, the reinforcement of the material by the filler leads to much higher stress applied in early stage of deformation, thus contributing to a fast crack propagation. Nevertheless, also in this case the coefficient of variance is within common limits since many cracks or crack supporting sites exist in close vicinity in all testing specimens. At medium filler content, a number of stress concentrating sites is formed, however, they are statistically not too close to each other. Therefore in some specimens the sites are more homogeneously distributed and their distance is larger than critical crack length, while small inhomogeneities may occur in the others leading to a more favouring situation for fast crack growth. The deformation in

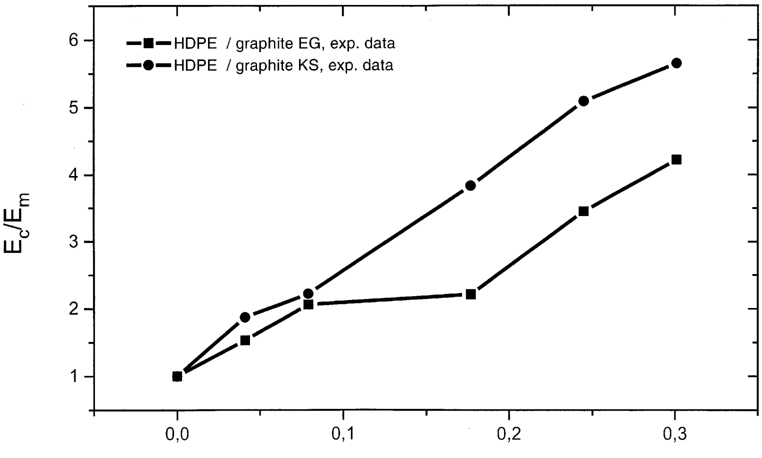

Fig. 9. Relative Young's modulus of elasticity (E_c/E_m) of the graphite EG (■) and graphite KS (●) filled HDPE graphite on the volume filler content (ϕ_f).

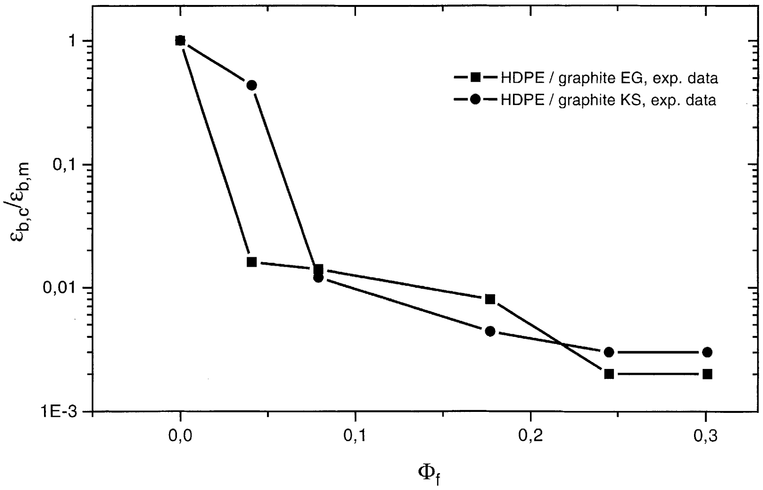

Fig. 10. Relative elongation at break ($\varepsilon_{b,c}/\varepsilon_{b,m}$) of the graphite EG (■) and graphite KS (●) filled HDPE graphite on the volume filler content (ϕ_f).

Table 5
Coefficiences of variance of Young's modulus (cv_E), elongation at break (cv_{ε_u}) and stress at break (cv_{σ_u}) of HDPE/graphite EG and HDPE/graphite KS composites

w_f	$cv_E{}^a$ (%)	$cv_{\varepsilon_u}{}^a$ (%)	$cv_{\sigma_u}{}^a$ (%)	$cv_E{}^b$ (%)	$cv_{\varepsilon_u}{}^b$ (%)	$cv_{\sigma_u}{}^b$ (%)
0	6	3.2	8.1	6	3.2	8.1
0.091	3	89.1	60.7	3.6	59.5	58.2
0.167	4	59.8	47.5	2.3	36.8	71.3
0.333	2.8	19.7	2.6	6.1	17.5	2.2
0.43	6.5	13.4	1.4	5.3	10.4	1.2
0.5	8	18.8	2.0	4.6	14.0	4.7

w_f is weight portion of the filler.

[a] HDPE/graphite EG composites.

[b] HDPE/graphite KS composites.

former specimens may be rather high while in the latter case the specimens will break at low deformation. Therefore, not only the coefficient of variation of measurement is extremely large but the set of experimental values consist of two groups, one with low deformation and another one where deformation was measured. This effect is more significant for smaller particles of graphite KS.

3.5.3. Stress at break

Stress at break depends on the filler concentration by a more complex way as seen in Fig. 11. In this case we have to consider the reinforcing effect of the filler leading to an increase of the tensile stress values with increasing filler content on the one hand, and the orientational strengthening occurring for semicrystalline polymers at high deformation on the other hand. The latter effect is indirectly negatively influenced by the filler presence by a steep decrease of the deformation so that orientation of the matrix cannot occur. At low filler contents, the deformation is low enough to prevent the orientation but the reinforcing effect of the filler presence is marginal. Therefore an initial decrease of tensile strength has been observed. With the increase in the filler content, the reinforcing effect is more pronounced while further decrease in deformation has no additional effect on orientation.

4. Conclusions

Electrical conductivity measurements showed that different types of graphite have a different influence on the percolation concentration of composites. The percolation filler concentration was found to be lower in semicrystalline matrix (HDPE) compared to amorphous matrix (PS). In an PS matrix percolation concentration does not depend on characteristics of the filler particles (particle size) while in semicrystalline matrix (HDPE) different values have been found for two graphite particles differing in surface area. Similar behaviour was observed for thermal conductivity and thermal diffusivity.

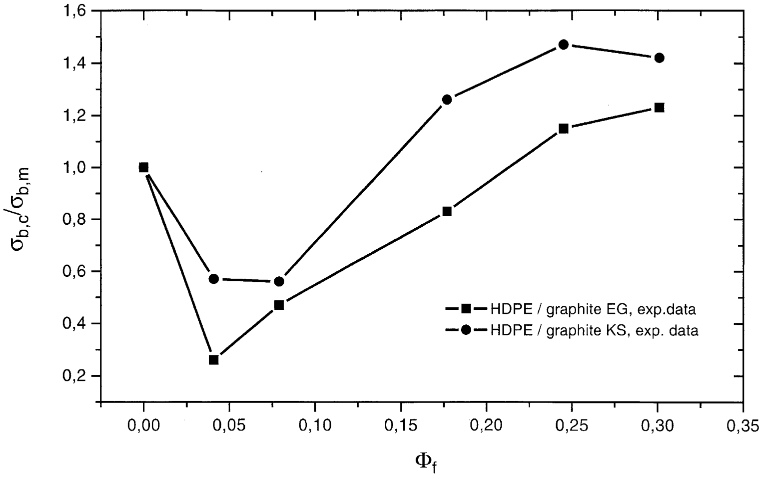

Fig. 11. Relative stress at break ($\sigma_{b,c}/\sigma_{b,m}$) of the graphite EG (■) and graphite KS (●) filled HDPE graphite on the volume filler content (ϕ_f).

Mechanical properties are influenced by reinforcing effect of the both fillers. The extent depends on the filler surface area, as indicated by increase in Young's modulus and decrease in elongation at break data.

Acknowledgements

The authors are grateful to Slovak grant agency for the financial support of this research (grant VEGA no. 2/1060/21).

References

[1] Ezquerra TA, Kulescza M, Balta-Calleja FJ. Synth Metals 1991;41:915.

[2] Navarro J, Roig A, Noguera P, Vicente F, Vilaplana J, López J. J Mater Sci 1994;29:4064.

[3] Blaszkiewicz M, McLachlan DS, Newnham RE. Polym Engng Sci 1992;32:421.

[4] Klason C, McQueen DH, Kubát J. Macromol Symp 1996;108:247.

[5] Bigg DB. Adv Polym Sci 1995;119:1.

[6] Chodák I, Krupa I. J Mater Lett 1999;18:1457.

[7] Lux F. J Mater Sci 1993;28:285.

[8] Sundstrom DW, Lee YD. J Appl Polym Sci 1972;16:3159.

[9] Bujard P, Munk K, Kuehnlein G. In: Tong TW, editor. Thermal conductivity 22. Lancaster, Basel: Technomic Publishing; 1994. p. 711–22.

[10] Jančář J. Plasty a Kaučuk 1990;27:289 [in Czech].

[11] Barta Š, Bielek J, Dieška P. J Appl Polym Sci 1997;64: 1552.

[12] Agari Y, Uno T. J Appl Polym Sci 1986;32:5705.

[13] Agari Y, Ueda A, Nagai S. J Appl Polym Sci 1993;49: 1625.

[14] Wunderlich B. Macromolecular physics II. New York: Academic Press; 1973.

[15] Nielsen R. Mechanical properties of polymers and composites 2. New York: Marcel Dekker; 1974.